Asymmetric Magnetization Switching in Perpendicular Magnetic Tunnel Junctions: Role of the Synthetic Antiferromagnet's Fringe Field

M. Lavanant, P. Vallobra, S. Petit-Watelot, V. Lomakin, A.D. D Kent, J. Sun, S. Mangin

Asymmetric Magnetization Switching in Perpendicular Magnetic Tunnel Junctions: Role of the Synthetic Antiferromagnet's Fringe Field

M. Lavanant,[1] P. Vallobra,[1] S. Petit Watelot,[1] V. Lomakin,[2] A.D. Kent,[3] J. Sun,[4] and S. Mangin[1,*]

[1]*Institut Jean Lamour, CNRS-UMR 7198, Université de Lorraine, 2, allée Guinier, F-5400 Nancy, France*
[2]*Center for Memory and Recording Research, University of California San Diego, 9500 Gilman Dr., La Jolla, California 92093-0401, USA*
[3]*Center for Quantum Phenomena, Department of Physics, New York University, 726 Broadway, New York, New York 10003, USA*
[4]*IBM T.J. Watson Research Center, IBM, 1101 Kitchawan Rd, Rt 13 Yorktown Heights, New York 10598, USA*

(Received 19 September 2018; revised manuscript received 21 December 2018; published 25 March 2019)

The field- and current-induced magnetization reversal of a Co-Fe-B layer in a perpendicular magnetic tunnel junction (pMTJ) is studied at room temperature. The magnetization switching probability from the parallel (*P*) state to the antiparallel (AP) state and from AP to *P* is found to be asymmetric. We observe that this asymmetry depends on the magnetic configuration of the synthetic antiferromagnetic (SAF). The state diagram and the energy landscape are compared for two SAF configurations. We conclude that the asymmetry is due to the inhomogeneity of the fringe field generated by the SAF. Our study highlights the role of the reference-layer fringe field on the free layer's energy barrier height, which has to be carefully controlled for memory applications.

DOI: 10.1103/PhysRevApplied.11.034058

I. INTRODUCTION

Current-induced manipulation of magnetization has been a subject of great interest since the prediction of spin transfer torque (STT) by Berger [1] and Slonczewski [2] in 1996. It has led to an innovative magnetic memory technology, namely spin-transfer torque magnetic random access memories (STT MRAM). Such devices are composed of magnetic tunnel junctions with electrodes exhibiting a strong perpendicular magnetic anisotropy (pMTJs) [3–6]. In these devices, the switching current is directly proportional to the energy barrier for thermally activated magnetization reversal [6,7]. Indeed, devices composed of materials with large perpendicular magnetic anisotropy (PMA) have been shown to combine both a good thermal stability and exhibit efficient current-induced switching [6–8]. To further improve a STT MRAM device, the switching energy and the switching time still need to be reduced [9,10], both of which depend on the energy barrier. The study and the characterization of the energy barrier is, therefore, crucial for improving the performance of STT MRAM.

Magnetic tunnel junctions are made of a thin insulating layer sandwiched between a free magnetic layer that can be switched and a reference layer. The latter acts as a spin polarizer for the current and gives rise to a dipolar field with a strong out-of-plane component. This magnetic field, also called a fringe field, may create an asymmetry in the magnetization reversal of the free layer [11]. In order to reduce this effect, "synthetic antiferromagnetic" structures (SAF) have been used to reduce the fringe field. The SAF is composed of two magnetic layers antiferromagnetically coupled through a nonmagnetic layer [12–14]. These layers' magnetizations are antiparallel and thus have a net magnetization close to zero and, to a first approximation, the average fringe field emitted by the SAF is also close to zero. However, the free layer still experiences a dipolar field associated with the SAF, as one layer of the SAF is closer to the free layer than the other. Moreover, the shape and the size of the device also influence the fringe field value and homogeneity [15–17].

Here, the role of the fringe field from the SAF on the free layer switching is studied. First, the probability of nonswitching for the free layer as a function of the voltage and magnetic field switching is obtained. The latter provides information on the energy barrier to thermally activated magnetization switching. The respective effects of a compensated SAF (antiparallel magnetized layers) and a saturated SAF (parallel magnetized layers of the SAF) on the switching probability and the switching state diagram are investigated.

II. EXPERIMENTS

A $[Co(0.25\ nm)/Pt(0.8\ nm)]_{14}$/Ru (0.9 nm)/Co (0.3mn)/$[Co(0.25\ nm)/Pd(0.8\ nm)]_4$/Co(0.25 nm)/Pt(0.8 nm)/

*stephane.mangin@univ-lorraine.fr

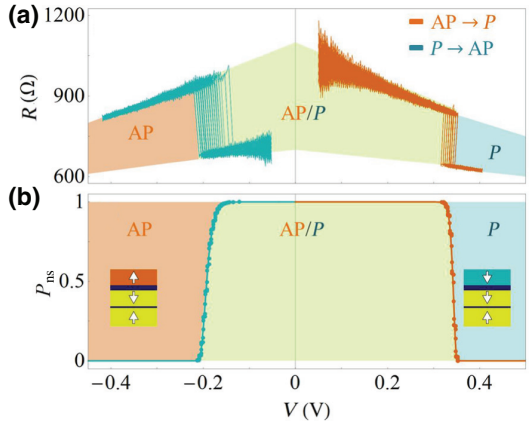

FIG. 1. Switching distribution for a 70×100 nm^2 pMTJ with a compensated SAF for an applied field $\mu_0 H = -30$ mT. (a) Resistance as a function of the applied voltage for voltage close to the AP to P transition (orange) and close to the P to AP (blue) for 1000 voltage sweeps and (b) nonswitching probabilities deduced from (a).

Co(0.25 nm)/Ta(0.3 nm)/Co-Fe-B(1.3 nm)/MgO(0.9 nm)/Co-Fe-B(0.8 nm)/ capping sample is grown by dc magnetron sputtering. The Co-Fe-B (0.8 nm) is the free layer and the Co (0.3mn)/[Co(0.25 nm)/Pd(0.8 nm)]$_4$/Co (0.25 nm)/Pt(0.8 nm)/Co(0.25 nm)/Ta(0.3 nm)/Co-Fe-B(1.3 nm) is the reference layer. The layers are separated by a MgO tunnel barrier. The reference layer is antiferromagnetically coupled through the Ru (0.9 nm) to the [Co(0.25)/Pt(0.8 nm)]$_{14}$ pinning layer. The reference layer and the pinning layer together form a SAF layer. We are interested in the switching behavior of the free layer magnetization between its two stable states, parallel (P) and antiparallel (AP) to the reference layer. The SAF is made to have an antiparallel alignment of the reference and the pinning layers in order to decrease the fringe field. However, in this study, to test the influence of the fringe field, we also consider the case where they are parallel. We call these configurations, respectively, "compensated" (AP) and "saturated" (P). Let us first consider the case when the SAF is compensated. All measurements presented in this paper are performed at room temperature.

Figure 1(a) shows the resistance of the pMTJ as a function of the voltage for the AP to P transition (orange) and the P to AP (blue) for numerous sweeps. There is a distribution of switching voltages. From these data, the probability of nonswitching as a function of the voltage as shown in Fig. 1(b) can be determined [16]. Our aim is to deduce the energy barrier associated with each transition from the corresponding probability of nonswitching as has been discussed in Ref. [18].

In order to do so, a single energy barrier $\Delta E(H)$ representing the thermal stability of a tunnel junction is considered between the two stable states [19]. Starting from the Landau-Lifshitz-Gilbert (LLG) equation describing the motion of the magnetization [20,21], it is possible to include the thermal fluctuation contribution based on the pioneering works of Néel [22] and Brown [23]. It has been shown that the effect of the voltage can be considered as an effective temperature [24,25]. Following the same idea, the nonconservative term of the STT is considered as an effective temperature in the LLG equation. Koch found then that the experimental values of STT-driven transition probabilities in spin valves were in good agreement with this theory [26]. The switching probability in MTJs can then be theoretically found using the same models. Values of the parameters needed to characterize the STT switching in MTJs can be found in the literature. *Ab-initio* calculations have shown that in MTJ, the STT nonconservative torque depends linearly on the applied voltage in pMTJs [27] and this has also been measured and verified experimentally [28,29].

This leads us to the expression of the nonswitching probability $P_{\rm ns}$ in a MTJ that follows for a voltage V sweeping with a rate r (10 V/s) experiment at fixed field $H_{\rm app}$

$$P_{\rm ns}(V, H_{\rm app}) = \exp\left[-\frac{1}{\tau_0 r}\int_0^V \exp\left(-\frac{\Delta E_0}{k_B T} \times \left(1 - \frac{H_{\rm app} - H_{\rm off}}{H_{\rm sw0}}\right)^{\eta}\left(1 - \frac{v}{V_{\rm sw0}}\right) dv\right)\right],$$

where $1/\tau_0$ is the attempt frequency of the switching (we have chosen 1 GHz), ΔE_0 is the energy barrier of the transition, and η is a parameter depending on the geometry and the switching type, taken here as $\eta = 3/2$ [19]. $H_{\rm sw0}$ and $V_{\rm sw0}$ are, respectively, the zero-temperature switching field and the switching voltage and $H_{\rm off}$ is, in the first approximation, the mean value of the average perpendicular fringe field. This equation is set under three main hypotheses: the measurement is quasistatic, the conservative part of the STT is neglected, and the Slonczewski spin torque is considered as an effective temperature.

The voltage sweepings presented in Fig. 1 are repeated for different fixed fields and using the expression of the probability of nonswitching, we obtain the dependence of the energy barrier of each transition as a function of the applied field $\Delta E(H_{\rm app}) = \Delta E_0/k_B T\{1 - [(H_{\rm app} - H_{\rm off})/H_{\rm sw0}]\}^{\eta}$. Figure 2(a) shows the energy barrier dependence as a function of the applied field for the two SAF configurations, compensated on the left (low fringe field) and saturated on the right (large fringe field). Figure 2(b) displays the corresponding state diagrams obtained by recording the switching voltage as a function of the applied field for both transitions and both configurations as described in Refs. [30–32]. Insets are schematics of the stack magnetic configurations. The results presented in Fig. 2 are obtained for a 70×100 nm^2 junction, but similar results

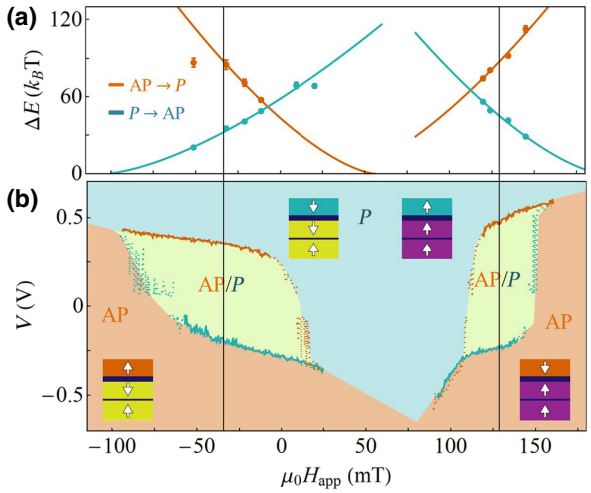

FIG. 2. (a) Evolution of the energy barrier for the AP to P transition (orange) and P to AP (blue) transitions as a function of the applied field with a compensated or a saturated SAF. (b) Evolution of the switching voltage for the AP to P transition (orange) and P to AP (blue) transitions as a function of the applied field with a compensated or a saturated SAF. The inset shows sketches of the P and AP states for the two SAF magnetic configurations (compensated and saturated).

are obtained for various junction sizes, from 60×80 nm^2 to 100×240 nm^2 (not shown).

For both configurations of the SAF, the state diagram presents an off-set field that we link in a first approximation to the average perpendicular component of the fringe field. We define $\mu_0 H_{\rm off}$ as the central value of the field hysteresis loop for no voltage. We obtain $\mu_0 H_{\rm off} = -30$ mT in the compensated configuration and $\mu_0 H_{\rm off} = 120$ mT in the saturated one. Their positions are noted in Fig. 2 as the vertical black lines. The evolution of the energy barrier as a function of field can be fitted by the above expression, as shown in Fig. 2(a). We observe that the energy barriers for P to AP and AP to P transitions vs applied field vary in opposite senses: they have opposite signs of their slopes for both SAF configurations. They also cross at a certain field. At this field, the energy barriers' switches from P to AP and from AP to P are equal. We expected that the latter field would correspond to the applied field that compensates the average fringe field, which is clearly not the case.

Both state diagrams presented in Fig. 2(b) are centered around the net off-set field value $\mu_0 H_{\rm off}$. However, there is an asymmetry of the switching voltages between the two transitions. The switching voltage from AP to P is larger than from P to AP. This effect is clearly seen in Fig. 1 as the measurement is done close to $H_{\rm off}$. We clearly observe that the nonswitching probabilities also have different dependencies on the voltage.

TABLE I. Stack parameters used for the FASTMAG simulations, the anisotropy constant K, the saturated magnetization M_S, the exchange coupling, and the damping.

Layers	K (J m^{-3})	M_S (A m^{-1})	A_x (J m^{-1})	$\alpha(-)$
1 & 2	$7.2{\cdot}10^5$	$10.5{\cdot}10^5$	$1.3{\cdot}10^{-11}$	0.01
3 & 4	$3{\cdot}10^5$	$3.5{\cdot}10^5$	$1.3{\cdot}10^{-11}$	0.01

A strong effect of the SAF magnetic state is observed in both the voltages and field-driven switchings. In the saturated SAF state, the state diagram width is reduced by two thirds and the switching voltages are shifted toward larger positive values for the AP to P transition. These observations indicate that the asymmetry in switching voltages and energy barriers cannot be described with a simple macrospin model, thus we use micromagnetic simulation to describe our experiments.

III. MODELING

The software FASTMAG developed at University of California San Diego [33] is used to study the switching process of the free layer at a given applied voltage, a given applied field, and zero temperature. This software uses a finite element method to solve the LLG equation. We compute a 60×80 nm^2 MTJ. We also consider a zero fieldlike torque and a coefficient of the Slonczewki term $a_V = 6.37 \times 10^3$ A m^{-1} V^{-1} [34]. The thickness resolution is 1 nm. We also consider the [Co|Pd] and [Co|Pt] multilayers to be one single block. The free layer (1), the barrier layer (gap), and the 1.3-nm Co-Fe-B layer (2) are set to be 1 nm thick each, the Co (0.3mn)/[Co(0.25 nm)/Pd(0.8 nm)]$_4$/Co(0.25 nm)/Pt(0.8 nm)/Co(0.25 nm) layer (layer 3) is set to be 5 nm thick, and the [Co(0.25 nm)/Pt(0.8 nm)]$_{14}$ layer (layer 4) is set to be 15 nm thick. The surface exchange coupling between the upper SAF layer and the reference layer is set to 1.242×10^{-3} J m^{-2}, and that between the two layers of the SAF is set to -1.242×10^5 J m^{-2}. The remaining stack parameters are shown in Table I [34,35]:

As already demonstrated, in order to reproduce the experimental state diagram using an analytical or numerical modeling, the uniaxial symmetry needs to be broken. In the present computation, we introduce a tilt of 0.6° in the magnetocrystalline anisotropy axis that is sufficient to break the uniaxial symmetry [32]. We are able to follow the magnetic configurations during the STT-driven magnetization switching, as seen in Figs. 3(c)–3(f). This allows us to compare the nucleation points of the reversal depending on the transition. In the case of the compensated SAF, the nucleation point depends on the transition: it occurs at an edge for the P to AP transition [Fig. 3(c)] and at the center of the layer for the AP to P transition [Fig. 3(d)]. In the case of the saturated SAF, the nucleations for both transitions occur at the edge of the sample [Figs. 3(e) and 3(f)].

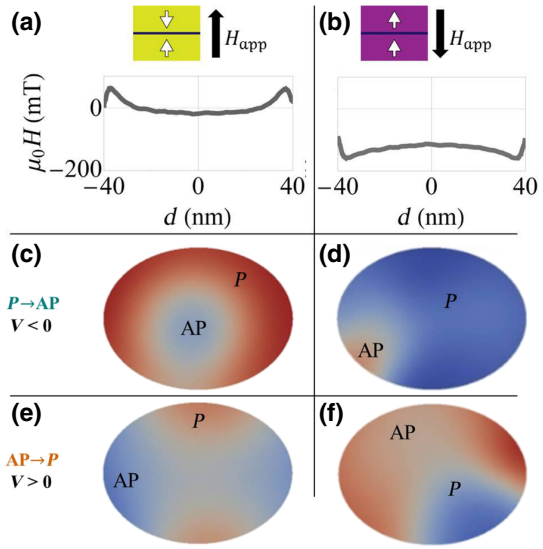

FIG. 3. (I) Micromagnetic simulations of the reference layers' fringe field of a 60×80 nm^2 element obtained from FASTMAG simulations at the free layer position for (a) the compensated SAF (blue) and (b) saturated SAF (orange) configurations. (II) Micromagnetic configuration of the nucleation process for the P to AP (first line) and AP to P (second line) STT-driven switching in the (a) compensated SAF (AP blue, P red) and (b) "no SAF" (AP red, P blue) configurations.

The strength of the dipolar field as a function of the distance from the center of the sample is also plotted in Figs. 3(a) and 3(b) for both SAF states and both transitions. We observe that the strength of the fringe field depends on the configuration of the SAF as intuited before. Also, in both SAF configurations, the stray field is inhomogeneous along the width of the junction. Even in the compensated case [Fig. 3(a)], it is close to zero at the center of the junction and higher at its edges. Since we show in Fig. 3 that the fringe field has a strong influence on the phase diagram, we claim that the peak in the fringe field at the edges of the sample can explain the asymmetry in the energy barrier of the transitions.

IV. CONCLUSION

The influence of the fringe field from the synthetic antiferromagnet on the switching behavior is shown experimentally by measuring the switching probability of the P to AP and AP to P transitions. The observed asymmetry between the two transitions cannot be explained by the presence of a homogeneous fringe field from the SAF. We demonstrate, thanks to micromagnetic simulations, that this asymmetry observed in quasistatic measurements is likely associated with inhomogeneities of the fringe field of the SAF at the edge of the sample. Similar asymmetry has been reported in the "nanosecond" dynamic switching regime for perpendicular MTJ [36]. Those inhomogeneities favor domain nucleation in certain areas of the free layer depending on the transition.

ACKNOWLEDGMENTS

Research at NYU was supported by Grant No. NSF-DMR-1610416. Research in Nancy was supported by the ANR-NSF COMAG project, Grant No. ANR-13-IS04-0008-01, by the ANR-Labcom LSTNM project Grant No. ANR-13-LAB2-0008, and by the French PIA project "Lorraine Université d'Excellence", Grant No. ANR-15-IDEX-04-LUE. Experiments were performed using equipment from the TUBE Davm funded by FEDER (EU), Grant No. ANR -14-IDEX-0001, Région Grand Est and Metropole Grand Nancy.

[1] L. Berger, Emission of spin waves by a magnetic multilayer traversed by a current, Phys. Rev. B **54**, 13 (1996).
[2] J. C. Slonczewski, Current-driven excitation of magnetic multilayers, J. Magn. Magn. Mater. **159**, L1 (1996).
[3] D. C. Worledge, G. Hu, P. L. Trouilloud, D. W. Abraham, S. Brown, M. C. Gaidis, J. Nowak, E. J. O'Sullivan, R. P. Robertazzi, J. Z. Sun, and W. J. Gallagher, Switching distributions and write reliability of perpendicular spin torque, MRAM IEDM (2010).
[4] S. Ikeda, K. Miura, H. Yamamoto, K. Mizunuma, H. D. Gan, M. Endo, S. Kanai, J. Hayakawa, F. Matsukura, and H. Ohno, A perpendicular-anisotropy CoFeB–MgO magnetic tunnel junction, Nat. Mater. **9**, 721 (2010).
[5] L. Thomas, G. Jan, J. Zhu, H. Liu, Y.-J. Lee, S. Le, R.-Y. Tong, K. Pi, Y.-J. Wang, D. Shen, R. He, J. Haq, J. Teng, V. Lam, K. Huang, T. Zhong, T. Torng, and P.-K.g Wang, Perpendicular spin transfer torque magnetic random access memories with high spin torque efficiency and thermal stability for embedded applications, J. Appl. Phys. **115**, 172615 (2014).
[6] B. S. Tao, D. L. Li, Z. H. Yuan, H. F. Liu, S. S. Ali, J. F. Feng, H. X. Wei, X. F. Han, Y. Liu, Y. G. Zhao, Q. Zhang, Z. B. Guo, and X. X. Zhang, " Perpendicular magnetic anisotropy in Ta|$Co_{40}Fe_{40}B_{20}$|$MgAl_2O_4$ structures and perpendicular CoFeB|$MgAl_2O_4$|CoFeB magnetic tunnel junction, Appl. Phys. Lett. **105**, 102407 (2014).
[7] S. Mangin, D. Ravelosona, J. A. Katine, M. J. Carey, B. D. Terris, and Eric E. Fullerton, Current-induced magnetization reversal in nanopillars with perpendicular anisotropy, Nat. Mater. **5**, 210 (2006).
[8] S. Mangin, Y. Henry, D. Ravelosona, J. A. Katine, and Eric E. Fullerton, Reducing the critical current for spin-transfer switching of perpendicularly magnetized nanomagnets, Appl. Phys. Lett. **94**, 012502 (2009).
[9] A. D. Kent and D. C. Worledge, A new spin on magnetic memories, Nat. Nanotechnol. **10**, 187 (2015).
[10] D. Sander, S. O. Valenzuela, D. Makarov, C. H. Marrows, E. E. Fullerton, P. Fischer, J. McCord, P. Vavassori, S. Mangin, and P. Pirro, The 2017 magnetism roadmap, J. Phys. D: Appl. Phys. **50**, 36 (2017).
[11] M. Gottwald, M. Hehn, D. Lacour, T. Hauet, F. Montaigne, S. Mangin, P. Fischer, M.-Y. Im, and A. Berger,

Asymmetric magnetization reversal in dipolar-coupled spin valve structures with perpendicular magnetic anisotropy, Phys. Rev. B **85**, 064403 (2012).

[12] Y. Kawato, M. Futamo, and K. Nakamoto, Perpendicular magnetic recording medium and magnetic storage apparatus, U.S. Patent No. US2002/0 028 356 A1 (2002).

[13] M. J. Carey, Y. Ikeda, N. Smith, and K. Takano, Dual-layer perpendicular recording media with laminated underlayer formed with antiferromagnetically coupled films, U.S. Patent No. US2003/0 022 023 A1 (2003).

[14] A. M. Shukh, E. W. Singleton, S. Khizroev, and D. Litvinov, Perpendicular recording medium with antiferromagnetic exchange coupling in soft magnetic underlayer, U.S. Patent No. US2002/0 028 357 A1 (2002).

[15] D. B. Gopman, D. Bedau, S. Mangin, C. H. Lambert, E. E. Fullerton, J. A. Katine, and A. D. Kent, Asymmetric switching behavior in perpendicularly magnetized spin-valve nanopillars due to the polarizer dipole field, Appl. Phys. Lett. **100**, 062404 (2012).

[16] L. Cuchet, B. Rodmacq, S. Aufret, R. C. Sousa, I. L. Prejbeanu, and B. Dieny, Perpendicular magnetic tunnel junctions with a synthetic storage or reference layer: A new route towards Pt- and Pd-free junctions, Nat. Sci. Rep. **6**, 21246 (2016).

[17] D. B. Gopman, D. Bedau, S. Mangin, E. E. Fullerton, J. A. Katine, and A. D. Kent, Switching field distributions with spin transfer torques in perpendicularly magnetized spin-valve nanopillars, Phys. Rev. B **89**, 134427 (2014).

[18] H. Liu, D. Bedau, J. Z. Sun, S. Mangin, E. E. Fullerton, J. A. Katine, and A. D. Kent, Dynamics of spin torque switching in all-perpendicular spin valve nanopillars, J. Magn. Magn. Mater. **358**, 233 (2014).

[19] R. Skomski, J. Zhou, R. D. Kirby, and D. J. Sellmyer, Micromagnetic energy barriers, J. Appl. Phys. **99**, 08B906 (2006).

[20] E. M. Lifshitz and L. D. Landau, Theory of the dispersion of magnetic permeability in ferromagnetic bodies, Phys. Z. Sowietunion **8**, 53 (1935).

[21] T. L. Gilbert, A lagrangian formulation of the gyromagnetic equation of the magnetic field, Phys. Rev. **100**, 1243 (1955).

[22] L. Néel, Théorie du traînage magnétique des ferromagnétiques en grains fins avec application aux terres 5 cuites, Ann. Geophys. **5**, 99 (1949).

[23] W. F. Brown, Thermal fluctuations of a single-domain particle, Phys. Rev. **130**, 5 (1963).

[24] S. Urazhdin, N. O. Birge, W. P. Pratt Jr., and J. Bass, Current-Driven Magnetic Excitations in Permalloy-Based Multilayer Nanopillars, Phys. Rev. Lett. **94**, 14 (2003).

[25] Z. Li and S. Zhang, Magnetization dynamics with a spin-transfer torque, Phys. Rev. B **68**, 024404 (2003).

[26] R. H. Koch, J. A. Katine, and J. Z. Sun, Time-Resolved Reversal of Spin-Transfer Switching in a Nanomagnet, Phys. Rev. Lett. **92**, 088302 (2004).

[27] I. Theodonis, N. Kioussis, A. Kalitsov, M. Chshiev, and W. H. Butler, Anomalous Bias Dependence of Spin Torque in Magnetic Tunnel Junctions, Phys. Rev. Lett. **97**, 237205 (2006).

[28] J. C. Sankey, Y.-T. Cui, J. Z. Sun, J. C. Slonczewski, R. A. Buhrman, and D. C. Ralph, Measurement of the spin-transfer-torque vector in magnetic tunnel junctions, Nat. Phys. **4**, 67 (2008).

[29] S. Petit, N. de Mestier, C. Baraduc, C. Thirion, Y. Liu, M. Li, P. Wang, and B. Dieny, Influence of spin-transfer torque on thermally activated ferromagnetic resonance excitations in magnetic tunnel junctions, Phys. Rev. B **78**, 184420 (2008).

[30] S. Le Gall, J. Cucchiara, M. Gottwald, C. Berthelot, C.-H. Lambert, Y. Henry, D. Bedau, D. B. Gopman, H. Liu, A. D. Kent, J. Z. Sun, W. Lin, D. Ravelosona, J. A. Katine, Eric E. Fullerton, and S. Mangin, State diagram of nanopillar spin-valve with perpendicular magnetic anisotropy, Phys. Rev. B **86**, 014419 (2012).

[31] Ioan Tudosa, J. A. Katine, S. Mangin, and Eric E. Fullerton, Phase diagram for spin-torque switching in perpendicular anisotropy magnetic nanopillars, Appl. Phys. Lett. **96**, 212504 (2010).

[32] M. Lavanant, S. Petit Watelot, A. D. Kent, and S. Mangin, State diagram of a perpendicular magnetic tunnel junction driven by spin transfer torque: a power dissipation approach, J. Magn. Magn. Mater. **428**, 293 (2017).

[33] R. Chang, S. Li, M. Lubarda, B. Livshitz, and V. Lomakin, FastMag: Fast micromagnetic simulator for complex magnetic structures, J. Appl. Phys. **109**, 07D358 (2011).

[34] K. Bernert, V. Sluka, C. Fowley, J. Lindner, J. Fassbender, and A. M. Deac, Phase diagrams of mgo magnetic tunnel junctions including the perpendicular spin-transfer torque in different geometries, Phys. Rev. B **89**, 134415 (2014).

[35] D. C. Worledge, G. Hu, D. W. Abraham, P. L. Trouilloud, and S. Brown, Development of perpendicularly magnetized Ta|CoFeB|MgO-based tunnel junctions at IBM, J. Appl. Phys. **115**, 172601 (2013).

[36] T. Devolder, A. Le Goff, and V. Nikitin, Size dependence of nanosecond-scale spin-torque switching in perpendicularly magnetized tunnel junctions, Phys. Rev. B **92**, 224432 (2016).